Upper Critical Magnetic Field far above the Paramagnetic Pair-Breaking Limit of Superconducting One-Dimensional $Li_{0.9}Mo_6O_{17}$ Single Crystals

J.-F. Mercure,[1] A. F. Bangura,[1,2] Xiaofeng Xu,[1,3] N. Wakeham,[1] A. Carrington,[1] P. Walmsley,[1] M. Greenblatt,[4] and N. E. Hussey[1]

[1]*H.H. Wills Physics Laboratory, University of Bristol, Tyndall Avenue, BS8 1TL, United Kingdom*
[2]*RIKEN (The Institute of Physical and Chemical Research), Wako, Saitama, 351-0198, Japan*
[3]*Department of Physics, Hangzhou Normal University, Hangzhou 310036, China*
[4]*Department of Chemistry and Chemical Biology, Rutgers University, Piscataway, New Jersey 08854, USA*

(Received 20 January 2011; revised manuscript received 15 September 2011; published 4 May 2012)

The upper critical field H_{c2} of purple bronze $Li_{0.9}Mo_6O_{17}$ is found to exhibit a large anisotropy, in quantitative agreement with that expected from the observed electrical resistivity anisotropy. With the field aligned along the most conducting axis, H_{c2} increases monotonically with decreasing temperature to a value 5 times larger than the estimated paramagnetic pair-breaking field. Theories for the enhancement of H_{c2} invoking spin-orbit scattering or strong-coupling superconductivity are shown to be inadequate in explaining the observed behavior, suggesting that the pairing state in $Li_{0.9}Mo_6O_{17}$ is unconventional and possibly spin triplet.

DOI: 10.1103/PhysRevLett.108.187003 PACS numbers: 74.25.Dw, 72.15.Eb, 74.20.Rp, 74.70.Dd

Superconductivity in quasi-one-dimensional (q1D) conductors has attracted sustained interest from the theoretical community [1], largely due to the fact that under certain conditions, rare phenomena such as spin-triplet pairing [2–4] or the spin-singlet, spatially inhomogeneous Fulde-Ferrell-Larkin-Ovchinnikov (FFLO) state [5–7] may be realized. The organic conductors $(TMTSF)_2X (X = PF_6, ClO_4)$ have been most extensively studied in this regard, though the nature of their pairing state has not yet been fully determined. In $(TMTSF)_2PF_6$, the constant Knight shift across the superconducting (SC) transition T_c [8], together with the observed violation of the Pauli paramagnetic limit [9] supports triplet pairing, while in $(TMTSF)_2ClO_4$, a Knight shift suppression below T_c and the presence of line nodes [10] indicate collectively a *d*-wave, spin-singlet pairing state. The possible realization of the FFLO state in $(TMTSF)_2ClO_4$ at low T, as suggested by recent angular studies of H_{c2} [11], is also consistent with singlet rather than triplet pairing. Theoretically, the coexistence of spin-(SDW) and charge-(CDW) density-wave instabilities can lead to a complex phase diagram where both singlet and triplet phases lie in close proximity, with triplet pairing becoming dominant as repulsive interchain interactions are enhanced [3,12,13]. Intriguingly, the triplet state known to exist in the q2D perovskite superconductor Sr_2RuO_4 might also arise from repulsive interactions between q1D bands [14].

$Li_{0.9}Mo_6O_{17}$ (LiMO) is a transition metal oxide with q1D electronic properties. It is metallic at high T, semiconducting below a temperature 15 K $\leq T_{min} \leq$ 30 K and superconducting below $T_c \sim 2$ K [15]. Despite having a T_c higher than the $(TMTSF)_2X$ family, its SC properties have received little attention to date. While the presence of a density-wave (DW) transition in LiMO was initially discounted, recent magnetotransport data appear to suggest some form of DW gapping [16]. The precise nature of the DW however, and its relation to the superconductivity, has yet to be resolved. Finally, signatures of superconductivity have been found to emerge at high magnetic fields [16] in LiMoO crystals that are non-superconducting in zero-field, consistent with theoretical predictions for a q1D superconductor with triplet pairing [6,7].

Here, we report a detailed temperature and orientational study of H_{c2} in crystals that are superconducting in zero-field and extract $H_{c2}(T)$ for fields applied along the three crystallographic axes. With the field parallel to the zigzag chains ($\mathbf{H} \parallel b$), H_{c2} increases monotonically with decreasing temperature to a value 5 times larger than the usual Pauli paramagnetic limit. We show evidence that LiMoO is a strongly coupled superconductor in the clean limit. However, the large H_{c2} values can neither be explained wholly by the effects of strong coupling [17] nor by spin-orbit scattering as parameterized by the Werthamer-Helfand-Hohenberg (WHH) theory [18]. Such a finding points to the possibility that the low-field SC state in LiMO might also be a spin triplet.

Figure 1 presents zero-field resistivity $\rho(T)$ curves from 300 K down to 1.6 K (4.2 K) for $\mathbf{I} \parallel a, c$ ($\mathbf{I} \parallel b$), respectively, scaled to incorporate all three curves on the same set of axes. Full details of the samples and measurement techniques are given in the Supplementary Information (SI) [19]. On cooling from room temperature, $\rho(T)$ is metallic down to about 15 K, followed by a well-defined upturn and finally, superconductivity. The size of the resistivity upturn is much smaller than found in the (non-superconducting) crystals described in Ref. [16], consistent with the anticorrelation between T_c and the size of the resistivity upturn first reported by Matsuda *et al.* [20]. The

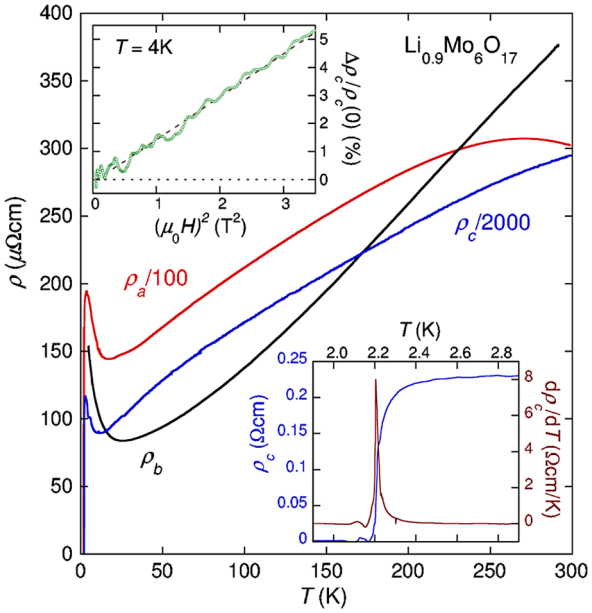

FIG. 1 (color online). Zero-field resistivity curves for $Li_{0.9}Mo_6O_{17}$ for $\mathbf{I} \parallel a$, b and c, scaled by 2000 (ρ_c) and 100 (ρ_a) for clarity. Note that the $\rho_b(T)$ trace only goes down to 4.2 K, as explained in the Supplementary Information [19]. Lower inset: Superconducting transition as seen in $\rho_c(T)$ (blue) and its temperature derivative $d\rho_c/dT$ (brown). Upper inset: c-axis magnetoresistance $\Delta\rho_c/\rho_c$ on the same single crystal at $T = 4$ K, i.e., just above T_c, plotted versus H^2 ($\mathbf{H} \parallel a$). The slope gives a measure of the in-chain mean-free-path (see text).

lower inset shows a blow-up of the c-axis resistive transition at T_c, the midpoint of which, as defined using the maximum in $d\rho_c/dT$, occurs at 2.2 K. The resistivity anisotropy extracted from this set of curves is 80:1:1600 (150:1:1600) for ρ_a:ρ_b:ρ_c at $T = 300$ K (4.2 K), respectively. This is almost 2 orders of magnitude larger than the anisotropies reported in the recent literature [21,22], highlighting the extreme care needed to isolate the individual current directions in such low-dimensional systems (see the SI section for further details [19]).

Figure 2 shows c-axis resistivity curves obtained in an 18 Tesla pumped ^{3}He cryostat with the field applied along a, b, and c, for temperatures between 0.33 and 2.40 K. The $\rho_c(H)$ curves for $\mathbf{H} \parallel b$ show an unusual broadening at intermediate temperatures, the origin of which is not understood at present. The large anisotropy in H_{c2} is apparent from inspection of the field scales in the three different panels. Field alignment for $\mathbf{H} \parallel b$ required an accuracy $<1°$ that was difficult to achieve in our ^{3}He system and higher H_{c2} values ($\mathbf{H} \parallel b$) were observed in a second set of measurements performed on the same crystal in a pumped ^{4}He system. The phase diagram for $H_{c2}(T)$ obtained from fixed-field temperature sweeps in the latter is shown in Fig. 3, where the open squares, two-tone squares and open circles refer to measurements performed with $\mathbf{H} \parallel a$, b, c respectively. Here, $H_{c2}(T)$ is determined by the maximum in the relevant derivative $d\rho_c/dT$ or $d\rho_c/dH$. As shown in the SI [19], choosing a different criterion does not change qualitatively the overall behavior, nor the anisotropy parameters. All data in Figs. 2 and 3 were corrected for the remnant field by symmetrizing with respect to positive and negative field values. Data for a second single crystal with a slightly lower T_c and $H_{c2}(0)$ are shown (for $\mathbf{H} \parallel b$ only) in [19].

From the initial slopes of the increase in $H_{c2}(T)$ below T_c (dashed lines in Fig. 3), we obtain $dH_{c2}/dT|_{T \le T_c}$ values of -1.5 T/K, -19.5 T/K and -0.5 T/K and a corresponding critical field ratio of 3:39:1 for $\mathbf{H} \parallel a$:b:c, respectively. According to anisotropic Ginzburg-Landau (GL) theory

$$\frac{H^i_{c2}}{H^j_{c2}} = \frac{\xi_i}{\xi_j} = \frac{\sqrt{\sigma_{ii}}}{\sqrt{\sigma_{jj}}} = \frac{\sqrt{\rho_{jj}}}{\sqrt{\rho_{ii}}}, \tag{1}$$

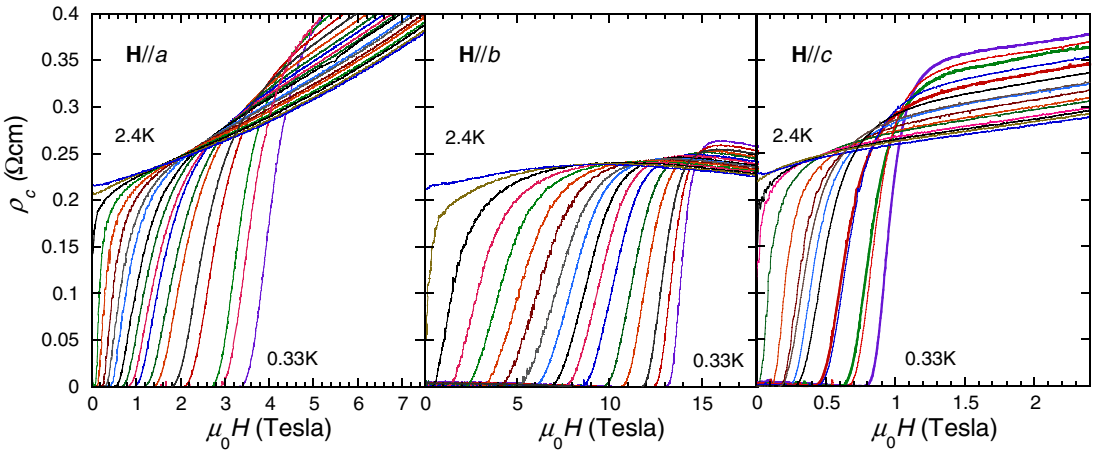

FIG. 2 (color online). Field sweeps of the c-axis resistivity of $Li_{0.9}Mo_6O_{17}$ in ~0.1 K steps for $\mathbf{H}$ aligned along the three crystallographic axes.

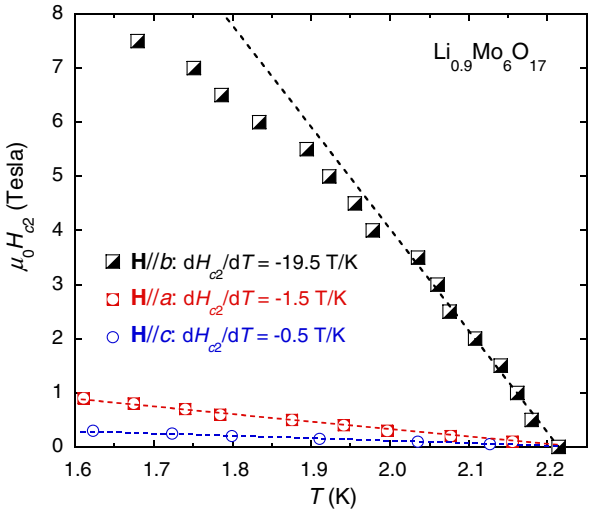

FIG. 3 (color online). Phase diagram for H_{c2} as a function of temperature for fields applied along the three crystallographic directions and temperatures down to 1.6 K obtained with the ^{4}He vapor pressure system.

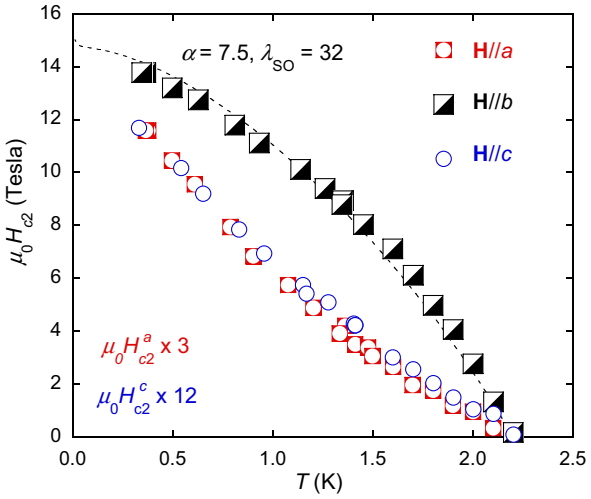

FIG. 4 (color online). Phase diagram for $H_{c2}(T)$ for temperatures down to 0.3 K obtained with the ^{3}He cryostat. The data were obtained from the field derivative of the magnetic field sweep curves shown in Fig. 2. Note that for $\mathbf{H} \parallel a$, c, the H_{c2} values have been normalized to emphasize the similarities of their T dependencies. The dashed line is a fit to the WHH theory with $\alpha = 7.5$ and $\lambda_{SO} = 32$ (see text for details).

where subscripts i, j refer to crystalline axes, superscripts i, j refer to the direction of the applied magnetic field, $\xi_{i,j}$ ($\propto v_{i,j}$) is the orientation dependent coherence length, $\sigma_{ii}/\sigma_{jj} (\propto v_{ii}^2/v_{jj}^2)$ is the anisotropy in the diagonal elements of the conductivity tensor and $v_{i,j}$ are the respective Fermi velocities. Squared, the SC anisotropy is approximately 9:1500:1, or 170:1:1500 when inverted. Note that these ratios are in excellent quantitative agreement with those (150:1:1600) obtained from the normal-state resistivity measurements.

A more complete $H_{c2}(T)$ phase diagram, extracted from the data plotted in Fig. 2, is shown in Fig. 4. (Note that the H_{c2} values for $\mathbf{H} \parallel a$, c have been rescaled in this plot). Using the (linearly) extrapolated zero-temperature values $H_{c2}(0)$ from the phase diagram and the equation

$$H_{c2}^i(0) = \frac{\Phi_0}{2\pi\xi_j(0)\xi_k(0)}, \qquad (2)$$

we obtain estimates for the three coherence lengths, $\xi_b(0) \simeq 300$ Å, $\xi_a(0) \simeq 100$ Å and $\xi_c(0) \simeq 25$ Å. Significantly, the interchain coherence lengths are both longer than the lattice spacing (or more precisely $2\xi_{a(c)}(0) > a(c) - d$ [23], where $a = 12.73$ Å and $c = 9.51$ Å are the a, c-axis lattice constants and $d \sim 3$ Å is the approximate width of the MoO_4 octahedra), implying the absence of Josephson coupling and a continuous phase of the SC order parameter across the chains. Hence, despite the extreme one-dimensionality of LiMO in the normal state, its superconductivity appears to be described satisfactorily using anisotropic-3D GL theory.

For a q1D spin-singlet superconductor with $\mathbf{H} \parallel$ chain, orbital pair-breaking is minimized (due to the small interchain electron velocities) and superconductivity can only be destroyed once the Zeeman energy arising from spin splitting of Cooper pairs exceeds the SC condensation energy. For an isotropic BCS superconductor, the Pauli limit is expressed as $\mu_0 H_P = 1.84 T_c \simeq 4.0$ T for $T_c = 2.2$ K. H_P can also be calculated independently [24] using actual values (see SI [19]) for the Pauli susceptibility $\chi_p (= 2.8 \times 10^{-6})$ and for the condensation energy U_c ($= 2.2$ mJ/mol, estimated from the specific-heat anomaly at T_c) obtained on crystals taken from the same batch and with similar T_c values. These give $\mu_0 H_p \simeq 3.1$ T for LiMO, i.e., comparable with the BCS value but still 5 times smaller than the measured $H_{c2}(0)$ for $\mathbf{H} \parallel b$.

According to WHH theory [18], spin-orbit scattering (e.g., at the Mo site) can act to limit Zeeman splitting and thus increase the value of H_{c2} beyond the usual Pauli limit. It is expressed using two dimensionless parameters, the Maki parameter α and the spin-orbit scattering λ_{SO}. The former is constrained through the expression $\alpha \simeq 0.528 dH_{c2}/dT|_{T \le T_c}$ ($\Leftarrow 7.5$ for the ^{3}He data), while $\lambda_{SO} = 2\bar{h}/3\pi k_B T_c \tau_{SO}$ ($= 32$) is determined from the best curve fit to the data, shown in Fig. 4 by a dashed line. The associated spin-orbit scattering time τ_{SO} can be converted to a mean-free-path ℓ_{SO} using the measured (in-chain) Fermi velocity [25]. For both data sets [i.e., from the ^{3}He (Fig. 4) and ^{4}He cryostats (Fig. 3)], $\ell_{SO} \sim 120$ Å.

An estimate for the transport mean-free path ℓ_0 can be obtained from the low-T interchain magnetoresistance

(MR). With $\mathbf{I} \parallel c$ and $\mathbf{H} \parallel a$, Boltzmann theory gives for a q1D metal in the weak-field limit

$$\frac{\Delta\rho_c}{\rho_c} = \left(\frac{ecB}{\hbar}\right)^2 \ell_0^2, \tag{3}$$

As shown in the top inset of Fig. 1, $\Delta\rho_c/\rho_c \propto B^2$ at low fields with a slope that yields $\ell_0 \sim 650$ Å at $T = 4$ K. According to the Abrikosov formula [26], $\tau_0/\tau_{SO} = (Z/137)^4$ ($Z = 42$ for Molydenum). Thus, one expects τ_{SO} to be $\sim$100 times longer than the transport lifetime τ_0, in marked contrast to what is obtained from the WHH parameters. Moreover, the diffusion constant obtained from the Maki parameter gives $\ell_0 < 1$ Å, showing clearly that WHH theory is inapplicable here (it is only truly valid in the dirty limit). It also shows that the spin-orbit scattering alone cannot account for the values of H_{c2} observed in LiMO.

Strong (e.g., electron-phonon) coupling can also act to reduce the effects of Pauli limiting through renormalization of the band splitting. Fits to the specific-heat anomaly yield a coupling constant $\lambda = 1.2 \pm 0.1$, intermediate between those of Nb and Pb. Even with this strength of coupling however, the magnitude of $H_{c2}(0)$ in LiMO is more than double the renormalized value (see SI [19] for more details) [17]. While one cannot exclude the possibility that the high H_{c2} found in LiMO is due to a combination of singlet pairing, strong-coupling superconductivity *and* strong spin-orbit scattering, it would require a precise combination of all of these effects to realize the present situation.

In a triplet superconductor, the spins of the Cooper pair can be coaligned, making the Pauli pair-breaking effect redundant. Triplet superconductivity is, however, extremely fragile and can easily be destroyed by impurities [27]. For our samples, $\ell_0 > 2\xi_b(0)$, i.e., within the clean limit, and while the FFLO state cannot be ruled out at the lowest temperatures and highest fields, significantly we find in LiMO, three of the key ingredients for realizing q1D triplet superconductivity: extreme one-dimensionality, a $H_{c2}(T)$ profile with minimal paramagnetic limiting and a long mean-free-path. The recent observation of scaling in the longitudinal b-axis MR in LiMO [16] provides compelling evidence that some form of DW develops below T_{min}. As discussed in the introduction, the nature of the DW fluctuations near T_c may ultimately determine the pairing state. In q1D systems close to a Peierls-type CDW instability, s-wave is the dominant pairing channel [28]. However structural [29], thermodynamic [20] and optical studies [30] have all failed to find evidence of a genuine phase transition in LiMO at $T = T_{min}$. We also find no evidence of a specific-heat anomaly at T_{min}, contrary to an earlier report [31]. This lack of evidence has lent support to the notion that the CDW instability in LiMO is in fact driven by *electronic* interactions [29], as is the case for strongly interacting coupled Luttinger liquids [32], with either singlet or triplet pairing competing for the ground state.

Finally, for $\mathbf{H} \perp b$, $H_{c2}(T)$ displays pronounced upward curvature, leading to a reduction in the SC anisotropy with decreasing temperature. A similar enhancement has been observed in $(TMTSF)_2PF_6$ and attributed to the formation of insulating (SDW) and SC domains at pressures approaching the SDW phase [33]. This model, in which H_{c2} is determined by the largest penetration depth perpendicular to the applied field, can account for the very similar H_{c2} values found for $\mathbf{H} \parallel a$ and $\mathbf{H} \parallel b$ in q1D $(TMTSF)_2PF_6$ as well as the upturn in H_{c2} for $\mathbf{H} \parallel c$. In LiMO however, there is no clear evidence for such an SDW phase at these temperatures and field scales and the anisotropy in H_{c2}, though reduced with decreasing temperature, always remains large.

An alternative explanation for the enhancement of H_{c2} is a field-induced reduction in the effective dimensionality of the electronic system, as observed in other q1D conductors [11,34–36]. For $\mathbf{H} \perp b$, the semiclassical motion of quasiparticles along, say, $\vec{k}$ oscillates with an amplitude $t_k/ev_F B$, where t_k is the $\vec{k}$-axis hopping parameter. (Note that even though $\rho_c(T)$ is nonmetallic at low-T, the positive, quadratic transverse MR shown in the inset to Fig. 1 indicates that coherent quasiparticles do exist in this temperature regime.) As B increases, the amplitude of the oscillatory interchain motion decreases [37]. This gradual confinement suppresses orbital pair-breaking and leads to an overall decrease in $v_{k(j)}$ and in turn ξ_k, which now becomes field dependent. As a result, H_{c2}^i increases with decreasing temperature. While this field-induced dimensional crossover will occur in *both* orthogonal field orientations, it is expected to happen at different field scales [38]. Moreover, it remains an open question whether this confinement process can lead to an enhancement of H_{c2} at fields well below the crossover field. In the case of triplet pairing, this field-induced dimensional crossover can lead ultimately to reentrant superconductivity [6,7], though in LiMO, such behavior has only been seen to date with the field aligned *parallel* to the molybdate chains and only in samples that do not superconduct in zero-field [16]. In the present batch of crystals, we observe a strong negative magnetoresistance for $\mathbf{H} \parallel b$, but as yet, no sign of reentrant superconductivity.

In conclusion, we have demonstrated the existence of a highly anisotropic, yet still three-dimensional SC state in LiMO with an anisotropy (near T_c) that is in excellent quantitative agreement with the measured normal-state electrical anisotropy. The magnitude of the b-axis upper critical field exceeds the usual Pauli limit by a factor of 5. We have shown that neither spin-orbit scattering nor strong-coupling superconductivity can account fully for this enhanced H_{c2} and thus have speculated that LiMO is a viable candidate for the realization of triplet superconductivity. Although the effective dimensionality of the

electronic state just above T_c is yet to be determined, LiMO displays all the hallmarks of a 1D Luttinger liquid at least above $T = T_{\min}$ [25,39], suggesting that the superconductivity may in fact have a higher dimensionality than the normal state out of which it condenses. In this case, pairing has to involve electrons on different chains, thus providing a test bed for theoretical claims that triplet pairing in q1D superconductors is stabilized in the presence of (repulsive) interchain interactions [3,12,13].

We thank J. F. Annett, P. Chudzinski, B. Gyorffy, R. H. McKenzie, J. Merino, and N. Shannon for stimulating discussions. This work was supported by the EPSRC (UK). X. X. acknowledges financial support from NSFC (No. 11104051), N. E. H. a Royal Society Wolfson Research Merit Award.

[1] V. J. Emery, Synth. Met. **13**, 21 (1986).
[2] D. Podolsky, E. Altman, T. Rostunov, and E. Demler, Phys. Rev. Lett. **93**, 246402 (2004).
[3] J. C. Nickel, R. Duprat, C. Bourbonnais, and N. Dupuis, Phys. Rev. Lett. **95**, 247001 (2005).
[4] K. Kuroki and Y. Tanaka, J. Phys. Soc. Jpn. **74**, 1694 (2005).
[5] A. I. Buzdin and V. V. Tugushev, Zh. Eksp. Teor. Fiz. **85**, 735 (1983); Sov. Phys. JETP **58**, 428 (1983).
[6] A. G. Lebed, Pis'ma Zh. Eksp. Teor. Fiz. **44**, 89 (1986).JETP Lett. **44**, 114 (1986).
[7] N. Dupuis, G. Montambaux, and C. A. R. Sa de Melo, Phys. Rev. Lett. **70**, 2613 (1993).
[8] I. J. Lee, S. E. Brown, W. G. Clark, M. J. Strouse, M. J. Naughton, W. Kang, and P. M. Chaikin, Phys. Rev. Lett. **88**, 017004 (2001).
[9] I. J. Lee, P. M. Chaikin, and M. J. Naughton, Phys. Rev. B **62**, R14 669 (2000).
[10] J. Shinagawa, Y. Kurosaki, F. Zhang, C. Parker, S. E. Brown, D. Jérome, J. B. Christensen, and K. Bechgaard, Phys. Rev. Lett. **98**, 147002 (2007).
[11] S. Yonezawa, S. Kusaba, Y. Maeno, P. Auban-Senzier, C. Pasquier, K. Bechgaard, and D. Jérome, Phys. Rev. Lett. **100**, 117002 (2008).
[12] K. Kuroki, R. Arita, and H. Aoki, Phys. Rev. B **63**, 094509 (2001).
[13] Y. Fuseya and Y. Suzumura, J. Phys. Soc. Jpn. **74**, 1263 (2005).
[14] S. Raghu, A. Kapitulnik, and S. A. Kivelson, Phys. Rev. Lett. **105**, 136401 (2010).
[15] M. Greenblatt, W. H. McCarroll, R. Neifeld, M. Croft, J. V. Waszczak, Solid State Commun. **51**, 671 (1984).
[16] Xiaofeng Xu *et al.*, Phys. Rev. Lett. **102**, 206602 (2009).
[17] J. P. Carbotte, Rev. Mod. Phys. **62**, 1027 (1990).
[18] N. R. Werthamer, E. Helfand, and P. C. Hohenberg, Phys. Rev. **147**, 295 (1966).
[19] See Supplemental Material at http://link.aps.org/supplemental/10.1103/PhysRevLett.108.187003 for details.
[20] Y. Matsuda, M. Sato, M. Onoda, and K. Nakao, J. Phys. C **19**, 6039 (1986).
[21] M. S. da Luz, C. A. M. dos Santos, J. Moreno, B. D. White, and J. J. Neumeier, Phys. Rev. B **76**, 233105 (2007).
[22] H. Chen, J. J. Ying, Y. L. Xie, G. Wu, T. Wu and X. H. Chen, Europhys. Lett. **89**, 67 010 (2010).
[23] N. E. Hussey J. R. Cooper, R. A. Doyle, C. T. Lin, W. Y. Liang, D. C. Sinclair, G. Balakrishnan, D. McK. Paul, and A. Revcolevschi, Phys. Rev. B **53**, 6752 (1996).
[24] F. Zuo, J. S. Brooks, R. H. McKenzie, J. A. Schlueter and J. M. Williams, Phys. Rev. B **61**, 750 (2000).
[25] F. Wang, J. V. Alvarez, S.-K. Mo, J. W. Allen, G.-H. Gweon, J. He, R. Jin, D. Mandrus, and H. Höchst, Phys. Rev. Lett. **96**, 196403 (2006).
[26] A. A. Abrikosov and L. P. Gor'kov, Zh. Eksp. Teor. Fiz. **42**, 1088 (1962); Sov. Phys. JETP **15**, 752 (1962).
[27] A. P. Mackenzie, R. K. W. Haselwimmer, A. W. Tyler, G. G. Lonzarich, Y. Mori, S. Nishizaki, and Y. Maeno, Phys. Rev. Lett. **80**, 161 (1998).
[28] H. Bakrim and C. Bourbonnais, Europhys. Lett. **90**, 27001 (2010).
[29] C. A. M. dos Santos, B. D. White, Yi-Kuo Yu, J. J. Neumeier, and J. A. Souza, Phys. Rev. Lett. **98**, 266405 (2007).
[30] J. Choi, J. L. Musfeldt, J. He, R. Jin, J. R. Thompson, D. Mandrus, X. N. Lin, V. A. Bondarenko, and J. W. Brill, Phys. Rev. B **69**, 085120 (2004).
[31] C. Schlenker, H. Schwenk, C. Escribe-Filippini, and J. Marcus, Physica (Amsterdam) **135B**, 511 (1985).
[32] D. Boies, C. Bourbonnais, and A.-M. S. Tremblay, Phys. Rev. Lett. **74**, 968 (1995).
[33] I. J. Lee, P. M. Chaikin, and M. J. Naughton, Phys. Rev. Lett. **88**, 207002 (2002).
[34] K. Behnia *et al.*, Phys. Rev. Lett. **74**, 5272 (1995).
[35] I. J. Lee, M. J. Naughton, G. M. Danner, and P. M. Chaikin, Phys. Rev. Lett. **78**, 3555 (1997).
[36] N. E. Hussey, M. N. McBrien, L. Balicas, J. S. Brooks, S. Horii, and H. Ikuta, Phys. Rev. Lett. **89**, 086601 (2002).
[37] L. P. Gor'kov and A. G. Lebed, J. Phys. (Paris), Lett. **45**, 433 (1984).
[38] A. Narduzzo, A. Enayati-Rad, P. J. Heard, S.L. Kearns, S. Horii, F. F. Balakirev, and N. E. Hussey, New J. Phys. **8**, 172 (2006).
[39] N. Wakeham, A. F. Bangura, X. Xu, J.-F. Mercure, M. Greenblatt, and N. E. Hussey, Nature Commun. **2**, 396 (2011).